DEVELOPMENT OF AN ALGORITHM TO REDUCE THE TOPOGRAPHICAL EFFECTS IN REFLECTED RADIANCE

YEAP ENG CHOON

UNIVERSITI SAINS MALAYSIA

2020

DEVELOPMENT OF AN ALGORITHM TO REDUCE THE TOPOGRAPHICAL EFFECTS IN REFLECTED RADIANCE

by

YEAP ENG CHOON

**Thesis submitted in fulfilment of the requirements
for the degree of
Doctor of Philosophy**

July 2020

ACKNOWLEDGEMENT

TABLE OF CONTENTS

LIST OF TABLES

Page

LIST OF FIGURES

Page

LIST OF SYMBOLS

θ	Surface incident angle.
θ_h	incident angle of horizontal surface
$\Delta\theta$	Difference in incident angle between target and model image
α	Surface slope angle.
$\emptyset$	Mean illumination angle
iz	Solar zenith angle
e	Exitance angle of tilted surface
e_h	Exitance angle of horizontal surface
ea	Slope aspect
ia	Solar azimuth angle
F	Sky viewing factor
L_c	Topographic corrected image in radiance
L	Radiance image with topographic effect
L_λ	Mean radiance of the image for band λ
L_r	Surface reflectance from direct irradiance
L_f	Surface reflectance from diffuse irradiance
L_a	Atmospheric scattered radiance
L_{toa}	Spectral radiance received by the sensor
b_λ	Exponential of diffuse sky irradiance
B_λ	Regression coefficients of the band reflectance
m_λ	rRgression coefficients of the band illumination
ρ_h^{dir}	Surface reflectance for direct irradiance

ρ_h^{dif}	Surface reflectance for diffuse irradiance
E^{dir}	Direct solar irradiance on horizontal surface
E^{dif}	Diffuse solar irradiance on horizontal surface
γ	Relationship between sloping and horizontal surface
I_{ext}	Extraterrestrial irradiance
D	Earth-Sun correction factor
$K_{1,2,3,4,5}$	Earth-Sun orbital constant parameter
Γ	Day angle for calculating Earth-Sun correction factor
d_n	Number of the day ranging from 1 to 365.
σ	Standard Deviation
N	Number of collected samples
x	Sample value
μ	Mean of all sample value
I_t	Total irradiance reaches the horizontal Earth surface (HSSI)
I_{ra}	Direct irradiance on horizontal surface
I_{fa}	Diffuse irradiance on horizontal surface
I_{toa}	Irradiance at the top of atmosphere
I_r	Rayleigh scattering component
I_a	Aerosol scattering component
I_g	Backscattering component
I_l	Direct solar irradiance on sloping surface
I_0	Diffuse solar irradiance on sloping surface
I_{fa}	Diffuse irradiance component of the HSSI
T_r	Transmission of Rayleigh scattering
T_a	Transmission of aerosol scattering

T_w	Transmission of water vapor
T_o	Transmission of ozone
T_u	Transmission of uniformly mixed gas (UMG)
T_n	Transmission of nitrogen dioxide
M_x	Band-specific multiplicative factor from Landsat 8 OLI handbook
Q_{cal}	Digital number of the satellite image
A_x	Band-specific additive rescaling factor from Landsat 8 OLI handbook
R	Surface albedo
R'	Surface reflection with topographical effect
λ_0	Lower boundary wavelength for Landsat 8 OLI spectral bandwidth
λ_1	Upper boundary wavelength for Landsat 8 OLI spectral bandwidth

LIST OF ABBREVIATIONS

6S	Second Simulation of Satellite Signal in the Solar Spectrum
AERONET	Aerosol Robotic Network
AOD	Aerosol Optical Depth
BRDF	Bidirectional Reflectance Distribution Function
DEM	Digital Elevation Model
DOS	Dark Object Subtraction
ETR	Extraterrestrial Irradiance
HSSI	Horizontal Surface Spectral Irradiance
MODTRAN	MODerate resolution atmospheric TRANsmission
NEqO	Near Equatorial Orbit
NRLSSI	Naval Research Laboratory Solar Spectral Irradiance
NRLTSI	Naval Research Laboratory Total Solar Irradiance
OLI	Operational Land Imager
RCS	Range Corrected Signal
RMSE	Root Mean Squared Error
SOLTICE	Solar Stellar Irradiance Comparison Experiment
SORCE	Solar Radiation and Climate Experiment
SIM	Spectral Irradiance Monitor
TOA	Top of Atmosphere
UMG	Uniformly Mixed Gas
SMARTS2	Simple Model of the Atmospheric Radiative Transfer of Sunshine

LIST OF APPENDICES

PEMBANGUNAN ALGORITMA UNTUK MENGURANGKAN KESAN

TOPOGRAFI DALAM PANTULAN SINARAN MATAHARI

ABSTRAK

Kesan topografi pada imej satelit bukanlah satu ralat tetapi sebaliknya distorsi yang disebabkan oleh geometri matahari dan permukaan. Permukaan yang menghadap ke arah matahari cenderung menjadi lebih cerah manakala permukaan yang jauh daripada matahari kebiasaannya lebih gelap. Kesan ini berkait rapat dengan sudut tuju matahari pada permukaan dan ia merupakan salah satu faktor utama yang meningkatkan variasi spektrum dalam imej satelit. Variasi spektrum boleh mengurangkan ketepatan imej satelit dalam applikasi seperti klasifikasi tidak diselia yang akan mengehadkan keupayaan aplikasi penderiaan jauh secara automasi. Ramai yang telah mencuba mengurangkan kesan topografi, tetapi kebanyakan kaedah yang digunakan adalah rumit dan memerlukan parameter yang banyak. Untuk menangani masalah ini, kami telah membangunkan algoritma yang dapat mengkuantitikan, mengurangkan dan memasukkan kesan topografi pada imej satelit dengan mengkaji hubunkait antara pancaran terus dan pancaran resap sinaran matahari. Algoritma ini diuji pada 11 imej satelit Landsat 8 dengan 120 titik sampel dari setiap imej untuk penilaian. Hasil yang diperolehi menunjukkan bahawa kaedah ini dapat mengurangkan kesan topografi, meningkatkan corak spektrum apabila pembetulan topografi dilakukan dan dapat meningkatkan persamaan antara imej satelit yang diambil pada tarikh yang berlainan apabila induksi topografi dilakukan.

DEVELOPMENT OF AN ALGORITHM TO REDUCE THE TOPOGRAPHICAL EFFECTS IN REFLECTED RADIANCE

ABSTRACT

Topographic effects in satellite images are not errors but distortions caused by the solar and surface geometry. Surfaces facing towards the Sun tend to be brighter while surfaces facing away from the Sun are generally darker. This effect is strongly related to solar surface incident angle, and it is one of the main factors that increase spectral variation in satellite images. Spectral variation may reduce accuracy, such as non-supervised classification, which can limit the capability of autonomous remote sensing applications. Many researchers have tried to reduce the effect of topography in the past with success; however, most of these methods are complicated and require many parameters. To address this problem, we developed algorithms that quantify, reduce, and induce topographical effects in satellite images by exploring the relationship between direct and diffuse solar irradiance. These algorithms use data from extraterrestrial irradiance, atmospheric profiles, digital elevation models, and radiative transfer models to calculate the amount of irradiance on Earth's surface to reduce distortions due to the topographic effect. The algorithm was tested on 11 Landsat 8 OLI satellite images assessed with 120 sample points each. The results demonstrate that this approach suppresses the topographic effect and improves spectral signatures and similarities between satellite images taken on different dates using topographic induction.

CHAPTER 1

INTRODUCTION

1.1   Overview

By the definition of Natsuyama et al. (1998), the topographic effect refers to topographic obscuration of terrestrial information on the surface observed, and it is affected mainly by the surface and solar geometry. Terrain with topographic irregularities cause variations in solar illumination on Earth's surface. As a result, surfaces facing the Sun receive more light and appear brighter than surfaces facing away from the Sun.

These effects allow humans to create the perception of three dimensions from a two-dimensional image by observing areas of shade and shadow (Wallach and Connel, 1953). However, in computer 'vision,' this effect may be misinterpreted as different types of object.

In general, satellite images are formed from the combination of three types of radiance as shown in Equation (1.1):

$$L_{toa} = L_r + L_f + L_a \hspace{3cm} (1.1)$$

where L_{toa} is the sum of the three radiances: L_r direct irradiance, L_f diffuse irradiance, and L_a atmospheric scattered radiance. The L_r contributes the most to total radiance, followed by reflectance of L_f and L_a as illustrated in Figure 1.1. In theory, if the contribution of these three radiance sources can be identified, then topographic improvement of the satellite image is relatively simple.
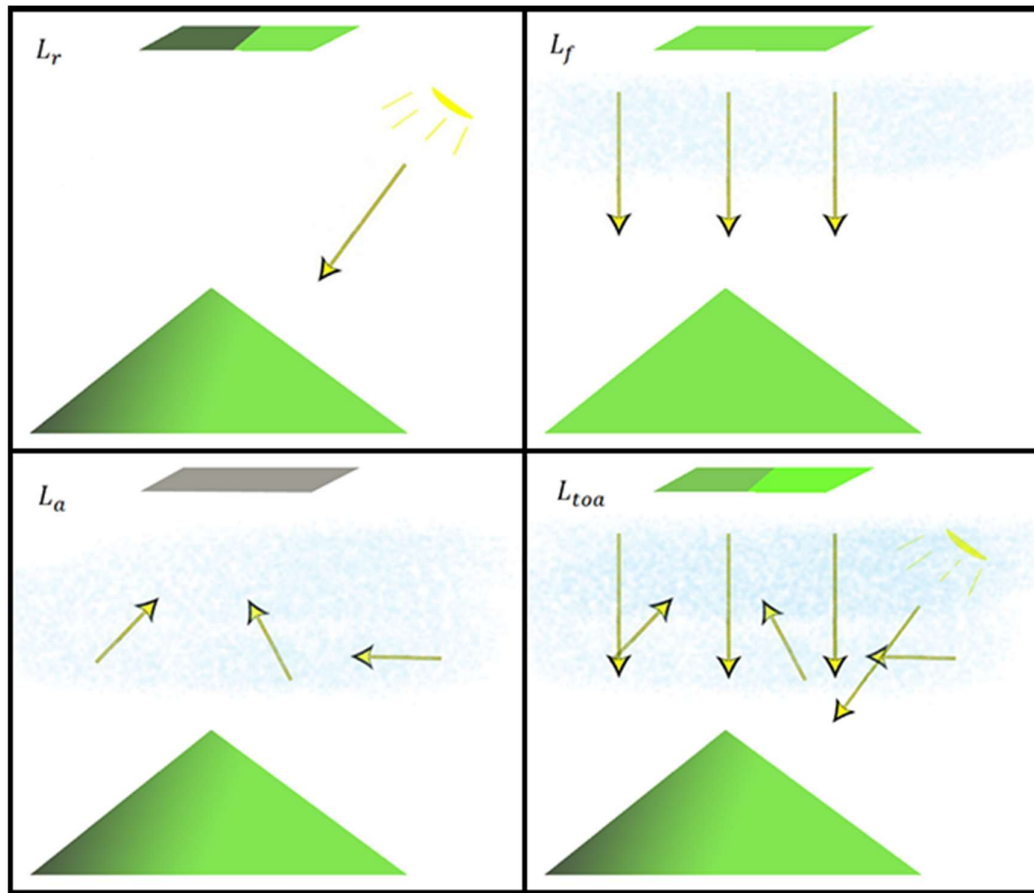
Figure 1.1   Illustration of the radiance reaching the satellite sensor

In Figure 1.1, the parallelogram at the top of each image represents two pixels on each side of the hill. Reflectance of L_r is the primary source of topographic effect. The parallelogram for L_r shows an obvious difference in colour tone, where the hill facing the Sun receives and reflects more sunlight compared to the hill facing away from the Sun, even though the reflection for both sides of the hill is the same. Changes in colour tone are related to the solar intensity that reaches the surface of the hill which can be calculated using the solar incident angle. As for L_f, the topographic effect from this radiance is less than the L_r. The L_f assumes that the source of irradiance is from isotropic scattering in the atmosphere; hence, the topographic effect for L_f can be calculated using the sky-view factor which was directly calculated using the slope

angle; depending on the wavelength, the shorter wavelengths experience more atmospheric scattering than longer wavelengths and thus contribute more L_f.

The third radiance, L_a is atmospheric noise which does not contain any information about the surface. Similar to the L_f, L_a is due to atmospheric scattering which occurs when the incoming solar irradiance and part of the scattered radiance is intercepted by the satellite. This radiance is isotropic (Dal Pai et al., 2016) which can be removed using the dark object subtraction (DOS) method (Wicaksono and Hafitz, 2017). The combination of the three radiances is what form the satellite images (L_{toa}). In order to retrieve the most information out of a satellite image, the contribution of these three radiance factors should be identified.

In this research, the contributions from the radiance are calculated using a radiative transfer model and a digital elevation model (DEM). Two algorithms were developed to correct the topographic effect in satellite images. The first algorithm was used to reduce the topographic effect on satellite images and extract the most information possible; the second algorithm induced the topographic effect to improve image analysis such as detection of changes in land use.

1.2   Background of the Study

Topographic distortion is one of the most complex problems in remote sensing due to its irregular distortion (Fan et al., 2018). In most remote sensing applications used to create images, reflection of solar irradiance is the primary useful signal received by the satellite; however, satellite images often contain irrelevant and distracting noise and distortions. Filtering this noise from satellite images is a challenging task because it requires pre-processing of data to reduce any errors and distortions inherited from the process of image acquisition (Sola et al., 2016). Common

errors and distortions include systematic and sensor errors, atmospheric effects, variable solar illumination, and topographic distortions which need to be resolved using various types of correction methods (Balthazar et al., 2012). Appropriate correction of distortion requires proper knowledge of the satellite image acquisition protocol.

In remote sensing, image acquisition is the process of obtaining a digital image from 'vision' sensors, such as a scanning device. Like most types of imaging sensors, the reflected photon that falls on to the charge coupled device (CCD) is converted into an electrical signal; an array of these signals is used to form the images. One of the most important parameters in forming a digital image is the light source. A consistent light source produces an image that contains the most information, while inconsistent lighting may saturate or underexpose the image, causing loss of valuable data from the image.

The Sun is the primary light source to illuminate Earth's surface for remote sensing. It provides convenient and stable irradiance throughout the day. Radiometric sensitivity of the imaging sensors is designed to work within the dynamic range of the Sun to capture the most information from Earth's surface. Combined with the Sun-synchronous low-Earth orbit, remote sensing satellites capture images of Earth with a consistent light source.

A Sun-synchronous orbit is able to maintain the same relationship with the Sun providing consistent illumination for each satellite pass; however, dynamic changes in Earth's atmosphere and the Sun's surface incident angle may still affect the light source which can be distorted in many ways. For example, the elliptical orbit of Earth around the Sun changes the Earth-Sun distance throughout the year, and the irradiance

may experience more or less atmospheric scattering and absorption, and changes in the surface solar incident angle affects the reflected intensity received by imaging devices. Many scientists address this problem as part of the 'topographic' effect in which similar objects exhibit small variations in spectral reflectance, especially on rough surfaces.

Research along these lines dates back to the 1980s when these early works were based on cosine correction. This method has improved over the past years. Six commonly used topographic correction methods are discussed in this thesis and include the cosine correction (CC), statistical empiric (SE), Minnaert correction (MC), Shepherd and Dymond correction (SD), sun-canopy-sensor (SCS), and path length correction (PLC) methods. Common problems with these topographic correction methods include over correction, which can greatly modify the spectral radiance value. To perform these corrections, many training samples are required; however, these correction methods do not return physical values and are difficult to automate. In this research, some of these problems are improved.

1.3   Statement of the Problem

Topographic effects are natural and inevitable. Because the Sun shines on the irregular surface of Earth, areas that face the Sun appear brighter, while areas facing away from the Sun appear dimmer. Changes in solar intensity are due to changes in the surface solar incident angle. The Sun rises in the East and sets in the West and the surface solar incident angle changes accordingly. The 23° tilt of Earth's rotational axis towards the Sun increases the complexity of the calculation of the solar geometry. Due to the nature of Earth's orbit around the Sun, the position of the Sun is almost never the same each time a remote sensing satellite passes over the scan surface. In this study,

5

four problems were identified through a literature study of topographic distortion: (1) every satellite image is uniquely affected by topography, (2) the topographic effect affects the accuracy of satellite images, (3) available physical topographic correction algorithms require many parameters which are often unavailable, and (4) topographic corrections not only reduce the topographic effect, they also remove some of the data from the satellite images.

For the first problem, the possible solar geometry during Landsat 8 satellite scanning over the study area for the year 2016 was plotted (Figure 1.2). The geometry of the Sun can be described with a two-axis geometry using the solar zenith angle and solar azimuth angle. The zenith angle is the angle between the zenith and the sun (sometimes describe as the solar elevation angle), while the azimuth angle is the angle between the sun and the North. Figure 1.2 shows the expected solar geometry described with solar zenith and azimuth angle every time the Landsat 8 OLI satellite passed through the upper atmosphere above Penang Island (Path 128, Row 056).

Changes in solar zenith and azimuth angle over the years indicate that the possibility of two satellite images taken under the same illumination condition is close to zero. In other words, every topographic distortion in a satellite image is unique. Due to the topographic effect, we recommend that spectral attributes, such as surface object identification and change detection, be topographically corrected in pre-processing (Fan et al., 2018).

Solar geometry during image acquisition of Penang Island
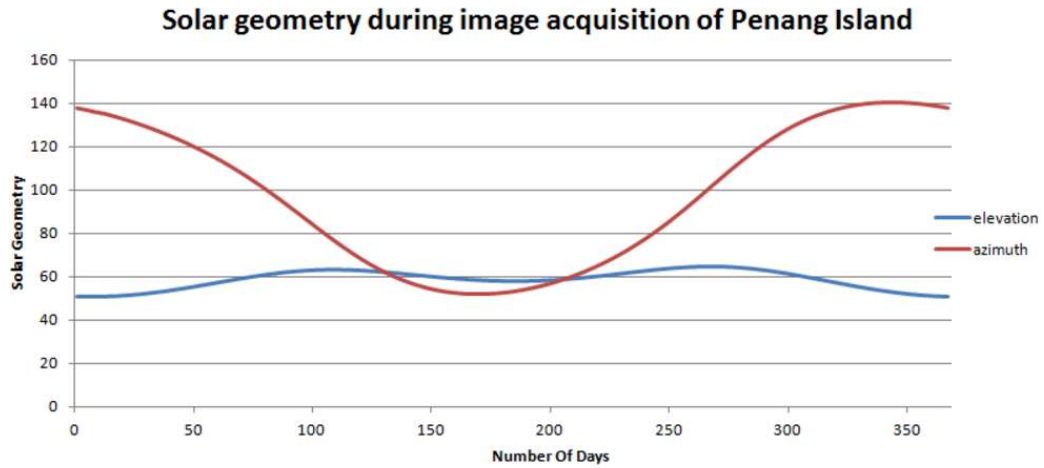
Figure 1.2 The expected solar geometry during the image acquisition on Penang Island scene (Path 128, Row 056) for Landsat 8 OLI.

Research has shown that changes in solar geometry do affect remote sensing data and its analysis (Ishihara et al., 2015; Zhang and Roy, 2016). Due to Earth's orbit around the Sun, it is inevitable that remote sensing using a satellite platform may experience changes in zenith and azimuth angle over the year. In Japan, the impact of sunlight conditions on the consistency of vegetation indices in croplands was studied. The results showed that vegetation indices decreased with decreasing solar zenith angle (Ishihara et al., 2015). In another study, during the years 1984 to 2011, a period of 27 years, the orbit for Landsat 5 changed with almost one hour difference in local solar time which induced solar zenith variations up to 10° (Zhang and Roy, 2016). These changes may result in a greater normalized difference vegetation index (NDVI) reaching up to 0.11 compared to the actual value in a given year during the operation (Zhang and Roy, 2016).

The third problem is that too many parameters are needed in topographic correction algorithm. Many have tried to improve satellite images by reducing the topography effect in the past with great successes; however, correcting topographical

effect is not a simple task. Compared with radiometric and atmospheric correction algorithms, relatively little interest has been shown in the topographical correction. Topographic corrections can be divided into two categories: empirical methods and semi-physical methods (Yin et al., 2018). As the name indicates, empirical methods improve satellite images empirically and do not require much ancillary data; however, the output of an empirical method does not have any physical meaning (Blesius and Weirich, 2005) which limits its application. Physical methods however provides output with physical values and can be done by modelling the propagation of solar radiation from the top of the atmosphere to the surface of Earth and back to the satellites' sensors. Topographic correction using physical methods generally requires a lot of data and possibly reduces the quality of the images, this preprocessing step is best to avoid unless absolutely necessary (Jensen, 2004).

Finally, topographic correction improves topographic variation due to surface and solar geometry, but loses some of the data. Slopes that face the Sun reduce brightness, while slopes that face away from the Sun become brighter after correction. Because the topographic correction affects every pixel in the image in a different way, it also reduces the radiometric quality. When a shaded surface is brought to light through correction, the digital number in that particular pixel is multiplied by a factor calculated by the algorithm which normalises the dark surface relative to its surroundings; however, the factor also reduce the radiometric resolution of that particular pixel producing a lower signal-to-noise ratio and increasing the probability of the 'salt and pepper' effect in shaded areas.

1.4   Objectives of the study

The objectives of this study are:

    I.   To model the solar irradiance distribution in Penang Island

    II.   To quantify the topographic effect

    III.   To develop an algorithm for topographic improvement

1.5   Significance of the study

This study offers a simplified method to correct distortions due to topographic effects in satellite images using fewer physical parameters than traditional correction methods. While others have had success with traditional methods, most of these approaches are complicated and require many parameters, making automated removal of topographic effect almost impossible (Shepherd and Dymond, 2003). In this study, a novel approach was used to address this problem by studying the relationship between direct and diffuse irradiance on a slope surface affected by the topographic effect. This approach enabled us to reduce some of the insignificant parameters in the equation such as land use data which are often unavailable. The algorithm used in this study delivered results with accuracy comparable to the traditional methods.

1.6   Scope of the study

During the study, certain limitations are stipulated for limiting the scope for this study. The scopes are:

1. Yearly average atmospheric profiles from local weather station nearby (Penang International Airport) were used to generate the regional atmospheric profile.

2. The atmospheric profile used in this study occurs from 0 km (Earth's surface) up to 16km where it holds 99% of the mass of atmosphere.

3. The study area for this research is confined to the Penang Island (N7°0' E99°45' – N4°05' E103°30') due to large amount of data consumption and data availability.

4. The satellite images used in the research came from Landsat 8 OLI with 30m in spatial resolution.

5. The DEM used in the research came from Alos Palsar with 12.5m in spatial resolution.

6. Atmospheric effects considered in this research were atmospheric absorption (water vapour, ozone, oxygen, carbon dioxide, and nitrogen dioxide), scattering, and multi-reflected radiance.

1.7   Thesis overview

The thesis is organized as follows:

Chapter 1 introduces the background of studies that have previously addressed the problem of topographic distortion in satellite images which motivates this study. The objectives of this study are presented in Chapter 1 and the significance addressed, followed by an outline of the scope of study.

In chapter 2, the methodology is addressed in detail. This chapter is divided into four sub-categories which explain data acquisition, primary data processing, topographic alteration algorithms, and assessment of the corrected results. The formulation of the topographic correction algorithm is also included in Chapter 2 together with the topographic induction algorithm.

In chapter 3, the methodology of the study was addressed in detail. This chapter was divided into four subcategories which explain the data acquisition, primary data processing, topographic alteration algorithm and the assessment of the topographic improved results. The formulation of the topographic correction algorithm was also included in this chapter together with the topographic induction algorithm.

Chapter 4 presents the results of the study and discusses limitations and implications. First, the results from horizontal surface spectral irradiance (HSSI) are reported. The HSSI estimated for the 11 Landsat 8 OLI images used is presented and assessed with the measured data. Issues related to the accuracy of the HSSI are discussed including the effects of atmospheric contamination and measurement tools. Next, the results of topographic corrected images are presented and discussed in detail. The results were assessed with 120 sample points for each bandwidth with satisfactory results. Finally, the results from topographic induction are discussed. One satellite image was used to simulate the 10 synthetic satellite images under different conditions. The synthetic images were assessed using the satellite images for stability and overall positive results, and the statistics of all results were reported.

Chapter 5 presents conclusions based on the results of the research performed and described in this thesis. The objectives achieved are highlighted and elaborated,

and suggestions for future work are recommended. This research found that the topographic effect in a satellite image is related to the ratio between direct and diffuse irradiance on the scanned surface. Surface illumination from direct solar irradiance is heavily influenced by the topographic effect due to changes in the incident angle. The second finding is that the difference between two images is related to the difference in surface incidence angle, $\Delta\theta$. Lower $\Delta\theta$ minimise the topographic effect between images, while higher $\Delta\theta$ increase differences between images.

CHAPTER 2

LITERATURE REVIEW

2.1   Introduction

In this literature review, six common topographic correction methods will be discussed along with seven assessment methods. Also, in physical modeling correction method, the involved model and algorithm used will be discussed. The model and algorithm include digital elevation model, extraterrestrial irradiance model, calculation of radiative transfer function, distribution of solar irradiance on rugged surface, bidirectional reflectance distribution function (BDRF) and conversion of digital number to surface radiance.

This chapter is divided into three sections where the first section reviewed the available topographic correction method. In the second section, the algorithm and model used in this study will be review and explain in detail. And in the last section, assessment of the correction method will be discussed.

2.2   Topographic correction methods

Multi-temporal studies in remote sensing requires the involve images to be homogenize in radiometric and geometric for better identification of the changes in the images. And topographic correction is one of the important steps in creating radiometric stable time series satellite images (Hantson and Chuvieco, 2011). Compared with the large amount of atmospheric correction algorithm, relatively little interest has been shown in the correction of topographic illumination.

According to Yin et al. (2018), topographic correction method can be categorized into two groups which are the empirical methods and physical method. In general, empirical methods such as cosine correction (CC) by Teillet et al (1982), Sun-

Canopy-Sensor with diffuse effect correction (SCS+C) by Soenen et al (2005), Statistical Empirical (SE) by Teillet et al (1982) and Minnaert (MIN) correction by Minnaert (1941) do not require much ancillary data (Sola et al., 2016). The procedure is easy to implement due to its simplicity. However, the output of the empirical methods does not have any physical meaning which limits its application (Blesius and Weirich, 2005).

Physical based method on the other hand taking into account of the propagation of solar irradiance from the top of atmosphere toward the ground and reflected back to the sensor along with other radiance such as atmospheric scattered radiance and multi surface reflectance. It employs radiative transfer model to calculate the energy arriving the surface of the Earth and applies cosine law to calculate surface incident angle (Huang et al., 2008). Using physical model avoids the empirical parameter thus achieve higher consistency and can overcome the overcorrection problem in cosine and Sun-canopy-sensor models (Dymond and Shepherd, 2003). Among the semi-physical methods are Sun-Canopy-Sensor (SCS), method proposed by Shepherd and Dymond (SD) and Path Length Correction method (PLC).

The six most common topographic correction methods are discussed in this chapter which are cosine correction (CC), Statistical Empirical (SE), Minnaert Correction (MIN), Sun-Canopy-Sensor method (SCS), Shepherd and Dymond's method (SD) and Path Length Correction (PLC).

2.2.1 Cosine Correction

One of the pioneers and widely discuss topographic correction methods is the cosine correction method (Hantson and Chuvieco, 2011; Sola et al., 2016) which can be expressed in Equation (2.1),

$$L_c = L(\cos a \,/ \cos \theta) \qquad (2.1)$$

Where: L_c is the corrected radiance.

L is the reflected radiance of the terrain.

α is the slope angle.

θ is the incident angle.

This algorithm is easily applicable due to its simplicity and does not require any external parameter. However, this method ignores the contribution of diffuse irradiance (Yin et al, 2018) and was repeatedly reported to have overcorrection under poor illumination (Shepherd and Dymond, 2003; Huang et al, 2008; Hantson and Chuvieco, 2011). A few alternative approaches were introduced after the cosine correction. Among the new algorithm are alternative algorithm proposed by Civco (1989) in Equation (2.2) which taking into account of the average illumination in the calculation.

$$L_c = L + L(\cos \emptyset - \cos \theta) / \cos \overline{\gamma \emptyset} \qquad (2.2)$$

Where: $\overline{\emptyset}$ is the mean illumination angle.

Both of the cosine correction and method proposed by Civco are wavelength independent which did not consider diffuse irradiance. To account for the transmission of different wavelength and diffuse irradiance, the C-correction was proposed. The C-

correction uses C_λ as the wavelength dependent empirical constant to account for the diffuse irradiance.

$$L_{c\lambda} = L_\lambda[(\cos iz - C_\lambda)/(\cos\theta - C_\lambda)] \qquad (2.3)$$

Where: iz is the incoming solar zenith angle.

C_λ is a wavelength dependent empirical constant which can be calculate using Equation (2.4).

$$C_\lambda = B_\lambda/m_\lambda \qquad (2.4)$$

Where: B_λ and m_λ are the regression coefficients of the band reflectance and illumination

2.2.2 Statistical Empirical

Statistical-Empirical (SE) method is one of the empirical methods that do not require much ancillary data. It is based on the assumption that the radiance varies due to the topography proportional in all wavelength (Sola et al., 2016).

$$L_{c\lambda} = L_\lambda - (\mathrm{a}\cos\theta + b_\lambda) + \overline{L_\lambda} \qquad (2.5)$$

Where: b_λ is the exponential of diffuse sky irradiance

$\overline{L_\lambda}$ is the mean radiance of the image for band λ.

2.2.3 Minnaert Correction

One of the most cited topographic correction on non-lambertian reflection is the Minnaert correction (Minnaert, 1941). In Equation (2.6), Minnaert constant $\mathcal{M}$ was used to present the weight of the anisotropic reflectance (Minnaert 1941; Bishop and Colby, 2002).

$$L_{c\lambda} = L_\lambda \left(\frac{\cos iz}{\cos \theta}\right)^{\mathcal{M}} \qquad (2.6)$$

Due to the dependency of Minnaert constant on wavelength, land cover type and phase angle, training samples are required for statistical regression to derive each Minnaert constant (Gao et al., 2016). The Minnaert constant has value between 0 to 1 with 1 is the perfect Lambertian reflector.

Further improvement of Minnaert method include the method proposed by Bishop and Colby (2002) which include slope angle in the calculation and method proposed by Gao (2016) namely Minnaert-E which include the effect of sky isotropic scattering. According to Gao's (2016) research, the performance of Minnaert-E is far better than its predecessor.

One of the disadvantages of this approach is the fact that Minnaert constant is land-cover and wavelength dependent which should be determined separately. This increase the complication of the application since land-cover maps are often unavailable (Hantson and Chuvieco, 2011).

2.2.4 Shepherd and Dymond correction method

Shepherd and Dymond (2003) proposed a new physical method which considered the Bidirectional Reflectance Distribution Function (BRDF) in reducing topographic effect which is much different from previous discussed method.

The physical method requires radiative transfer model to estimate the direct and diffuse irradiance on the surface. Sun angle and viewing geometries are both explicitly involved in the calculation. The general equation for describing the observed brightness is express in Equation (2.7).

$$L = \frac{\left(\rho_h^{dir} E^{dir}/\gamma\right) + \left(\rho_h^{dif} E^{dif}\right)}{\pi} \qquad (2.7)$$

Where: ρ_h^{dir} is the surface reflectance for direct irradiance.

ρ_h^{dif} is the surface reflectance for diffuse irradiance.

E^{dir} is direct solar irradiance on horizontal surface.

E^{dif} is diffuse solar irradiance on horizontal surface.

γ is the relationship between sloping and horizontal surface.

The proposed method firstly estimates the direct and diffuse irradiance on horizontal surface using 6S. After that, a DEM was used to calculate the incident angle for the slope surface followed by a cast shadow algorithm that was used with the known solar position to produce a binary shadow mask. In addition, the author also added a sky viewing factor (V) in the calculation to improve the estimation of the contribution from diffuse irradiance. The value of V can be calculate using in Equation (2.8) where the s is the slope angle.

$$V = \frac{1+\cos s}{2} \qquad (2.8)$$

However, the canopy structure was not accounted in this method which causing unsatisfactory topological correction in some cases (Ritchter et al., 2009, Yin et al., 2018). Suggested by Yin et al., (2018), the SD method is suitable for isotropy land cover which focuses on relative accuracy rather than biophysical parameter retrieval that focus on high absolute reflectance accuracy.

2.2.5 Sun-Canopy-Sensor (SCS)

Most of the topographic correction method discussed previously did not consider BRDF. One popular method to account the BRDF is the utilization of the Sun-Canopy-Sensor (SCS) correction which also pioneering method in BRDF correction (Yin et al., 2018). The expression of the SCS is shown in Equation (2.9). This method assumes that the main contribution factor of pixel-reflectance is from the sunlit canopy (Yin et al., 2018). Like cosine correction, pixel with large incident angle over slopes facing away from the Sun are likely to be over corrected (Huang et al., 2008).

$$L_c = \frac{L(\cos\alpha\cos iz)}{\cos\theta} \qquad (2.9)$$

One of the important disadvantages mentions by Yin et al (2018) is that the SCS correction does not consider the viewing angle effect. This may subsequently limit its application with narrow viewing angle. To improve the performance of the SCS correction, semi empirical parameter C (Soenen et al., 2005) was introduced to account for the diffuse irradiance and to reduce the overcorrection phenomenon namely SCS+C (Equation 2.10). Similar to the previous Minnaert constant ($\mathcal{M}$), C is a scene dependent parameter. Although many studies have adopted this method and achieved some good results (Thompson et al., 2018; Qiu et al., 2019), the SCS with improved C correction is a semi empirical method that is not suitable for multitemporal and multisensory comparison (Huang et al., 2008).

$$L_c = \frac{L(\cos\alpha)(\cos iz)}{\cos\theta + C} \qquad (2.10)$$

2.2.6 Path Length Correction (PLC)

A path length is defined as "distance between the top and the bottom of the canopy along with a direction relative to the canopy height" (Luisa et al., 2008). It is a critical variable that affect the radiative transfer within canopy (Yin et al., 2018) and has been applied to characterize three-dimensional canopy structure for leave area index (Yan et al., 2016; Hu et al., 2018). The path length was stretches in the up-slope direction while compresses in the down-slope direction which is a major factor causing the BRDF distortion (Yin et al., 2018).

Derivation of the path length correction by Yin et al (2018) consists of two major steps which the first step is to simplify a radiative transfer equation based on a few assumptions. The first assumption is that the canopy is illuminated only by collimated light while diffuse and surrounding reflected radiation is negligible; The second assumption is that radiance collected by the sensor is and only from single scattering of leaves while reflectance from soil and multiple scattering are ignored.

The second steps in the PLC are to formulate the path length over horizontal and sloping terrain. By substituting the calculated path length from the second step, the corrected reflectance can be obtained. The simplified expression of the PLC on horizontal surface are shown in Equation (2.11).

$$\rho_{PLC} = \rho_t \frac{S(\Omega_1) + S(\Omega_2)}{S_t(\Omega_1) + S_t(\Omega_2)} \tag{2.11}$$

Where: ρ_{PLC} is the corrected image.

P_t is the image observed reflectance.

$S(\Omega_1)$ is the path lengths along solar direction over flat terrain.

$S(\Omega_2)$ is the path lengths along viewing direction over flat terrain.

$S_t(\Omega_1)$ and $S_t(\Omega_2)$ are the counterpart for $S(\Omega_1)$ and $S(\Omega_2)$ over sloping terrain.

The path length correction method was tested against some topographic correction method on Landsat 8 OLI image with results similar to empirical parameter-based method (Yin et al., 2018). In summary, this correction method provides an efficient way to improve the terrain induced canopy BRDF distortion and return with good results especially over mountainous areas. However, this approach is only suitable for forested land cover. A good understanding of the land cover is required for estimating the path length in every image which will complicate the process of the correction.

2.2.7   Comparison between topographic correction methods

Table (2.1) shows the method discussed with the expression. A number of topography correction methods were made available in the past few decades. However, the performance of the topographic correction method was not standardized.

From the literature, the evaluation method used to evaluate the topographic correction method is different and not standardized which is not easily comparable (Sola et al., 2016; Hantson and Chuvieco, 2011). In addition, most of the study area from the literature are different with different in land cover, topography and solar geometry which have direct impact on the magnitude of reduction of topography effect. According to the study by Hantson and Chuvieco (2011), before the year 2011, most of the topographic correction method are not properly evaluated since these studies only consider image with good illumination condition and the impact of land covers was not commonly assessed. The first study which address this problem in the literature (Richter et al., 2009) which study the performance of different topography effect with different land cover. However, the study images were taken under

favorable illumination condition which naturally produce better results and did not
fully exhibit the full potential of topographic correction method.

Table 2.1   Summarize of the discussed topographic correction methods.

TOC	Expression	Author
Cosine Correction	$L_c = L(\cos a / \cos \theta)$	Teillet et al. (1982)
Civco's Method	$L_c = L + L(\cos \emptyset - \cos \theta)/\cos \emptyset$	Civco et al. (1989)
C-Correction	$L_{c\lambda} = L_\lambda[(\cos iz - C_\lambda)/(\cos \theta - C_\lambda)]$	Teillet et al. (1982)
Statistical-Empirical	$L_{c\lambda} = L_\lambda - (a\cos \theta + b_\lambda) + \overline{L_\lambda}$	Teillet et al. (1982)
Minnaert	$L_{c\lambda} = L_\lambda \left(\dfrac{\cos iz}{\cos \theta}\right)^{\mathcal{M}}$	Minnaert (1941)
Shepherd and Dymond	$L = \dfrac{\rho_h^{dir} E^{dir}/\gamma + \rho_h^{dif} E^{dif}}{\pi}$	Shepherd and Dymond (2003)
Sun-Canopy-Sensor	$L_c = \dfrac{L(\cos \alpha \cos iz)}{\cos \theta}$	Soenen et al. (2003)
Sun-Canopy-Sensor+C	$L_c = \dfrac{L(\cos \alpha)(\cos iz)}{\cos \theta + C}$	Soenen et al. (2003)
Path Length Correction	$\rho_{PLC} = \rho_t \dfrac{S(\Omega_1) + S(\Omega_2)}{S_t(\Omega_1) + S_t(\Omega_2)}$	Yin et al. (2018)

In another study (Hantson and Chuvioco, 2011), the authors used eight
topographic correction method to topographically improve 15 Landsat ETM image
and assess with two assessment procedure. The topography correction method involve
in this study are cosine correction, empirical-statistic, empirical statistic_NDVI, C-
correction, C-correction_NDVI, Minnaert with slope, Minnaert with slope_NDVI an
modified Minnaert.

15 Landsat images at the central part of Iberian. Peninsula with different solar geometric was topographically improve which return 120 results. The method used to assess these results are (1) calculating the changes in standard deviation of pixel value from the same land-cover over different slope and aspect and (2) measuring the temporal stability of a time series at individual pixels.

The results of this study show that empirical-statistic method and C-correction produce the best results in term of the homogeneity of different land cover. In term of temporal stability, Empirical-Statistic method proof to be superior among other method. However, the good result is only possible when the necessary parameters were estimated independently for each land cover (Gao et al., 2016). As a result, artifacts were form at the border of the land cover. The two main reason forming the artifacts are (1) due to higher number of mixing pixel and (2) different parameter was applied on each land cover which causes discontinuity between each classes of land cover (Hantson and Chuvieco, 2011).

To improve the topographic correction, a better resolution of DEM with topographically match with the satellite images and better separation between land-cover is necessary.

2.3   Physical topographic correction method

In this study, physical topographic correction method was used to reduce the topographic effect. This method was preferred due to the higher consistency and repeatability of this method. As discussed previously, a physical method modelled the propagation of the solar irradiance from the Sun to Earth and reflects to the satellite's sensors. The parameter required by physical methods are extensive. In the following

section, the main model used to calculate the required parameter will be discussed in detail. The discussed models include extraterrestrial irradiance model and radiative transfer model.

2.3.1 Extraterrestrial irradiance

Extraterrestrial irradiance is the irradiance measured at one astronomical unit (AU) from the Sun. An AU is the average distance between the Sun and Earth which is equivalent to 150 million kilometers. Some literatures refer the extraterrestrial irradiance as irradiance at the top of the atmosphere also known as air mass zero irradiance.

On the surface, the irradiance reaches the Earth's surface is known as surface irradiance. Surface irradiance mainly consists of surface reflected radiance, direct and diffuse solar irradiance. An accurate estimation of this irradiance is very crucial in this study as it directly affect the accuracy of the results. As mentioned in previous studies (Gao et al., 2016, Sola et al., 2016), a physical topographic correction method started with an extraterrestrial solar irradiance. Constant spectral solar irradiance was used in every radiative transfer model for calculating transmission of solar irradiance. From the literature (Coddington et al., 2016), neither the total nor spectral solar irradiance is constant despite the historical reference of solar irradiance as "constant solar irradiance".

Measurement of the extraterrestrial irradiance has started since the 70's with the commonly used irradiance model WRC81 publish by Neckel and Labs. Spectral solar irradiance models were used in variety of application among different disciplines. In particular, Gueymard (2004) describe the used of extraterrestrial solar irradiance to